Barium isotopic composition of the mantle: Constraints from carbonatites

Wang-Ye Li [a,b,*], Hui-Min Yu [a,b], Juan Xu [a], Ralf Halama [c], Keith Bell [d], Xiao-Yun Nan [a], Fang Huang [a,b,*]

[a] *CAS Key Laboratory of Crust-Mantle Materials and Environments, School of Earth and Space Sciences, University of Science and Technology of China, Hefei, Anhui 230026, China*

[b] *CAS Center for Excellence in Comparative Planetology, Hefei, Anhui 230026, China*

[c] *School of Geography, Geology and the Environment, Keele University, Keele, Staffordshire, ST5 5BG, UK*

[d] *Department of Earth Sciences, Carleton University, 1125 Colonel By Drive, Ottawa, Ontario K1S 5B6, Canada*

Text words: ~3700

Figures: 3

Tables: 3

Revised version submitted to GCA (June 12, 2019)

---

* Corresponding authors.

E-mail addresses: wyli@ustc.edu.cn (W.-Y. Li), fhuang@ustc.edu.cn (F. Huang).

Abstract

To investigate the behaviour of Ba isotopes during carbonatite petrogenesis and to explore the possibility of using carbonatites to constrain the Ba isotopic composition of the mantle, we report high-precision Ba isotopic analyses of: (1) carbonatites and associated silicate rocks from the only active carbonatite volcano, Oldoinyo Lengai, Tanzania, and (2) Archean to Cenozoic carbonatites from Canada, East Africa, Germany and Greenland. Carbonatites and associated phonolites and nephelinites from Oldoinyo Lengai have similar $\delta^{137/134}$Ba values that range from +0.01 to +0.03‰, indicating that Ba isotope fractionation during carbonatite petrogenesis is negligible. The limited variation in $\delta^{137/134}$Ba values from −0.03 to +0.09‰ for most carbonatite samples suggests that their mantle sources have a relatively homogeneous Ba isotopic composition. Based on the carbonatites investigated in this work, the average $\delta^{137/134}$Ba value of their mantle sources is estimated to be +0.04 ± 0.06‰ (2SD, n = 16), which is similar to the average value of +0.05 ± 0.06‰ for mid-ocean ridge basalts. The lower $\delta^{137/134}$Ba value of −0.08‰ in a Canadian sample and higher $\delta^{137/134}$Ba values of +0.14‰ and +0.23‰ in two Greenland samples suggest local mantle isotopic heterogeneity that may reflect the incorporation of recycled crustal materials in their sources.

Keywords: barium isotopes; carbonatites; mantle geochemistry; crustal recycling

1. Introduction

Stable isotopes are powerful tools for identifying crustal recycling into the mantle, primarily due to significant stable isotope fractionation at low temperatures or near the Earth's surface (e.g., Hoefs, 2018). Recent studies have already explored mass-dependent isotopic variations for heavy metals (Fe, Cu, Mo, Hg, U etc.) in different geochemical reservoirs and their use as geochemical tracers for a wide range of geological processes (see Teng et al., 2017). The Ba stable isotope system is potentially a sensitive tracer of crustal recycling because Ba is highly enriched in crustal rocks (average of 456 μg/g for the continental crust; Rudnick and Gao, 2014) and in pelagic and terrigenous marine sediments (average of 786 μg/g for the mean of global subducted sediments; Plank, 2014). By comparison, the depleted mantle (DM) and bulk silicate Earth (BSE) have average Ba contents of 1.2 μg/g (Salters and Stracke, 2004) and 7.0 μg/g (Sun and McDonough, 1989), respectively.

Barium has seven stable isotopes and the percent abundance of these isotopes is as follows: ^{130}Ba (0.11%), ^{132}Ba (0.10%), ^{134}Ba (2.42%), ^{135}Ba (6.59%), ^{136}Ba (7.85%), ^{137}Ba (11.23%), and ^{138}Ba (71.70%) (Eugster et al., 1969). Recent studies have demonstrated substantial Ba isotope fractionation among terrestrial samples and experimental precipitates (see review of Charbonnier et al., 2018). For example, measurements of granites, loess, glacial diamictites and river sediments show that the upper continental crust has highly variable $\delta^{137/134}Ba_{SRM3104a}$ values ($\delta^{137/134}Ba_{SRM3104a} = [(^{137/134}Ba)_{sample}/(^{137/134}Ba)_{SRM3104a} - 1] \times 1000$, where SRM3104a is a pure Ba standard solution from NIST) ranging from −0.47 to +0.35‰ (Nan et al., 2018), and

44 negative values down to ca. −0.5‰ were reported from marine/diagenetic barite (von
45 Allmen et al., 2010). If Ba isotopes are to be used as possible tracers for crustal
46 recycling, the Ba isotopic composition of the mantle reservoir needs to be defined. To
47 our knowledge, no Ba isotopic data are currently available for mantle peridotites, and
48 Ba isotopic data for mid-ocean ridge basalts (MORBs) have only recently been
49 reported in a single paper, with $\delta^{137/134}$Ba values that range from +0.02 ± 0.03‰ to
50 +0.11 ± 0.03‰ (Nielsen et al., 2018). The $\delta^{138/134}$Ba values published by Nielsen et al.
51 (2018) have been recalculated to enable comparison with the $\delta^{137/134}$Ba values used in
52 this study, i.e. $\delta^{137/134}Ba = 0.75 \times \delta^{138/134}Ba$ (Horner et al., 2015). Nielsen et al. (2018)
53 speculated that the limited variability in Ba isotopic composition of MORBs reflects
54 binary mixing between a "depleted MORB (D-MORB) mantle" with $\delta^{137/134}$Ba =
55 +0.11 ± 0.02‰ and an "enriched MORB (E-MORB) mantle" with $\delta^{137/134}$Ba = +0.02
56 ± 0.02‰, where the two end-member components were defined by the samples with
57 the lowest $^{87}Sr/^{86}Sr$ (0.7023) and the highest $^{87}Sr/^{86}Sr$ (0.7034) ratios, respectively.
58 However, D-MORBs with $^{87}Sr/^{86}Sr < 0.7024$ display $\delta^{137/134}$Ba values from +0.02 to
59 +0.11‰, overlapping with the range from +0.02 to +0.08‰ of E-MORBs with
60 $^{87}Sr/^{86}Sr > 0.7030$ (Nielsen et al., 2018). This feature suggests that the supposed Ba
61 isotopic difference between the depleted mantle and enriched mantle may not actually
62 exist.

63 In order to further investigate the Ba isotopic characteristics of the mantle, we
64 focus on igneous carbonatites, i.e. mantle-derived rocks containing >50% carbonate
65 minerals. They are generated through low-degree partial melting of carbonated mantle,

either as primitive melts or as parental carbonated silicate melts that undergo differentiation by liquid immiscibility and/or crystal fractionation (see reviews in Bell et al., 1998; Bizimis et al., 2003). Carbonatites can provide information on mantle geochemistry because: (1) they are widely distributed (>500 occurrences on all continents) with ages ranging from 3 Ga to present (Woolley and Kjarsgaard, 2008), (2) their petrogenesis is now considered by some researches to be closely linked to the global carbon cycle (e.g., Barker, 1996; Hoernle et al., 2002), and (3) they are sensitive indicators of thermal instabilities because they are near-solidus melts and can be associated with dynamic processes in the mantle (e.g., orogenic activity or mantle upwelling including plumes/hot spots; Woolley and Kjarsgaard, 2008; Ernst and Bell, 2010). In terms of isotopes, the radiogenic isotopic data of most young carbonatites (<200 Ma) plot within the fields of some ocean island basalts (OIBs), with values similar to the FOZO (focal zone), HIMU (high μ, where $\mu = {}^{238}U/{}^{204}Pb$) and EM1 (enriched mantle type 1) mantle components based mainly on data from OIBs (Bell and Tilton, 2001). Mixing between two of these components, HIMU and EM1, characterizes many of the carbonatites from East Africa (Bell and Tilton, 2002; Bell and Simonetti, 2010). By contrast, the depleted MORB mantle (DMM) plays little role in forming carbonatites (see figures in Rukhlov et al., 2015). These observations are more consistent with a model involving the generation of carbonatite melts from sub-lithospheric mantle rather than the lithosphere (Bell and Simonetti, 2010). Both the traditional C and O stable isotopes (e.g., Deines, 1989; Keller and Hoefs, 1995; Ray et al., 1999) and the non-traditional Li and B stable isotopes

88 (Halama et al., 2008; Hulett et al., 2016) have been analyzed in carbonatites to
89 document isotopic variations of their mantle sources and to monitor their temporal
90 evolution.

91 Carbonatites are ideal for investigating the Ba isotopic characteristics of the
92 mantle because they contain very high abundances of Ba (generally hundreds to tens
93 of thousands μg/g; e.g., Woolley and Kempe, 1989; Keller and Kraft, 1990).
94 Moreover, the extremely low viscosity (e.g., Genge et al., 1995) leads to rapid
95 migration of carbonatite melts to the surface, reducing the possible addition of Ba
96 from crustal assimilation. In this work, high-precision Ba isotopic data were obtained
97 of 19 well-characterized carbonatites. In addition, ten silicate rocks were analyzed
98 from Oldoinyo Lengai. The purpose of this work is to illustrate the behaviour of Ba
99 isotopes during carbonatite petrogenesis, and assess its significance in constraining
100 the Ba isotopic composition of their mantle sources.

101

102 ## 2. Samples

103 The carbonatite and associated silicate rock samples analyzed in this work are
104 from Canada, East Africa, Germany and Greenland, with ages that range from the
105 Archean to present. These samples have been well characterized with respect to
106 petrological, major and trace element, and Sr-Nd-Pb-Li-B-C-O-Mg isotopic aspects
107 (Schleicher et al., 1990; Tilton and Bell,1994; Bell and Simonetti, 1996; Simonetti et
108 al., 1997; Bell and Tilton, 2001; Halama et al., 2005, 2007, 2008; Klaudius and Keller,
109 2006; Rukhlov et al., 2015; Hulett et al., 2016; Li et al., 2016). Similar to the majority

of global carbonatites, the carbonatite samples studied here have Sr-Nd isotopic compositions similar to those of OIBs (Halama et al., 2008). Most of the samples have oxygen isotopic compositions that fall into the range of "primary" igneous carbonatites, although some samples show elevated $\delta^{18}O$ values, which are common post-emplacement features in altered carbonatites (Demény et al., 2004). The detailed petrological and geochemical features of the samples have been presented in previous literature (Halama et al., 2007, 2008, and references therein), and only a brief introduction about the samples is given here.

2.1. The 0 Ma carbonatites and silicate rocks from Oldoinyo Lengai, Tanzania

As Oldoinyo Lengai is the only active carbonatite volcano on Earth, it has played a key role in assessing the origin of carbonatite melts (see Bell and Keller, 1995). The generally accepted model for natrocarbonatite petrogenesis at Oldoinyo Lengai involves silicate-carbonatite immiscible separation from a parental carbonated, alkaline silicate melt (e.g., Freestone and Hamilton, 1980; Church and Jones, 1995; Keller and Spettel, 1995; Dawson, 1998; Brooker and Kjarsgaard, 2011). Additional magmatic processes described at Oldoinyo Lengai include fractional crystallization of carbonate minerals nyerereite [$Na_2Ca(CO_3)_2$] and gregoryite [$(Na_2, K_2, Ca)CO_3$] (e.g., Peterson, 1990; Gittins and Jago, 1998) as well as phenocryst assimilation and cumulate disruption (Mitchell and Dawson, 2012). Differentiation via carbonate-halide liquid immiscibility may also have occurred during eruption (Potter et al., 2017).

Klaudius and Keller (2006) defined three major structural units of Oldoinyo Lengai (i.e., *Lengai I*, *Lengai II A*, and *Lengai II B*) and discussed the petrogenetic relationship of silicate rocks and natrocarbonatites from each unit. Stratigraphic relationships and Sr-Nd-Pb isotopic data suggest that the combeite–wollastonite nephelinites (CWNs) and natrocarbonatites of *Lengai II B* are conjugate silicate and carbonatite melts produced by liquid immiscibility, unlike the phonolites of *Lengai I* and CWNs of *Lengai II A* (Klaudius and Keller, 2006). Samples studied here include: 1) natrocarbonatites (OL2, OL7, OL123, OL148 and OL259) and the petrogenetically related CWNs (OL624, OL788 and OL804) from the *Lengai II B* unit, and 2) silicate rocks not generated by liquid immiscibility (including phonolites OL440, OL442, OL450, OL503 and OL822 from the *Lengai I* unit as well as CWNs OL247 and OL803 from the *Lengai II A* unit). Li et al. (2016) found that the silicate rocks related to carbonatites by liquid immiscibility have different Mg isotopic compositions to other silicate rocks, implying significant Mg isotope fractionation during silicate-carbonatite liquid immiscibility. Comparison between the Ba isotopic compositions of these two types of silicate rocks can provide constraints on the behaviour of Ba isotopes during the generation of conjugate liquids.

2.2. Archean to Cenozoic carbonatites from Canada, East Africa, Germany and Greenland

The Archean carbonatite samples from the Dolodau and Lac Shorrt occurrences in Canada (2.7 Ga) are biotite-calcite carbonatites (DOD77, LSC20 and LSC108) and an

amphibole-biotite silicocarbonatite (DOD91). Proterozoic carbonatite samples from the Gardar igneous province, South Greenland, are calcite carbonatites (GR46, GR73 and GR74) from the Grønnedal-Ika complex (1.3 Ga). Phanerozoic carbonatite samples consist of a calcite carbonatite sample (K5) from the 17 Ma old Kaiserstuhl complex, Germany, and carbonatites with ages ranging from 138 to 13 Ma from the East African Rift (calcite carbonatites N1295, PH212, PH213, SU103 and HB, and a ferrocarbonatite DU365).

The 29 whole-rock samples investigated here for Ba isotopic compositions are the same powders as those studied previously for radiogenic and Li-C-O isotopic compositions (Halama et al., 2007, 2008, and references therein) as well as Mg isotopic compositions but only for the Oldoinyo Lengai samples (Li et al., 2016). On the basis of petrography and Li-C-O-Mg isotopic data (Halama et al., 2007, 2008; Li et al., 2016), post-emplacement alteration is negligible for all but three of the carbonatite samples from East Africa (i.e., N1295, DU365 and OL804). These three samples show signs of late-stage alteration (e.g., altered minerals or hydrothermal veins), and two of them (N1295 and DU365) have elevated $\delta^{18}O$ values (12.4‰ and 15.6‰) that lie outside the range of "primary" igneous carbonatites (see Fig. 5a in Halama et al., 2008).

3. Analytical methods

Barium isotopic analyses were performed at the University of Science and Technology of China, Hefei. All chemical procedures were carried out in an ISO-class

176 6 clean laboratory. Using screw-top Teflon beakers, the whole-rock powders were
177 dissolved in a combination of concentrated HF–HNO_3–HCl. Purification of Ba was
178 achieved by cation exchange chromatography with Bio-Rad 200–400 mesh
179 AG50W–X12 resin, following established procedures (Nan et al., 2015, 2018).
180 Sample solutions containing ~2 μg Ba were loaded onto the resin. The Ba recoveries
181 through column chemistry, based on analyses of Ba content in the elution collected
182 before and after the Ba cut, were >99%. The procedural blank was 2 ng Ba.

183 Barium isotopic measurements were carried out on a Neptune Plus multi-collector
184 inductively coupled plasma mass spectrometer (MC–ICP–MS), and a double-spike
185 technique was used to correct for instrumental mass bias. An appropriate amount of
186 the ^{135}Ba–^{136}Ba double spike with a ratio of 1.72 (m/m; Rudge et al., 2009) was added
187 to a portion of the purified sample solution containing ~100 ng Ba. The optimal range
188 of the proportion of double spike in the double spike-sample mixture is 0.43 to 0.60.
189 The "dry" plasma conditions (Aridus II desolvating nebulizer) were used to increase
190 sensitivity (~7V/100ng/g for ^{137}Ba). Barium isotopic analyses were conducted in a
191 low-resolution mode, with ^{134}Ba, ^{135}Ba, ^{136}Ba and ^{137}Ba collected simultaneously by
192 the L2, L1, C and H1 Faraday cups, respectively. ^{131}Xe and ^{140}Ce were also collected
193 by the L4 and H3 Faraday cups to correct the effects of isobaric interferences from Xe
194 and Ce. The background signals for ^{137}Ba (<0.005 V) were negligible relative to the
195 sample signals (~7 V).

196 The results are reported in $\delta^{137/134}$Ba values relative to the NIST Standard
197 Reference Material (SRM) 3104a, i.e. $\delta^{137/134}Ba = [(^{137/134}Ba)_{sample}/(^{137/134}Ba)_{SRM3104a} -$

198 1] × 1000. For comparison, all published $\delta^{138/134}$Ba values have been recalculated to
199 $\delta^{137/134}$Ba values by assuming mass-dependent fractionation following $\delta^{137/134}$Ba =
200 0.75 × $\delta^{138/134}$Ba (Horner et al., 2015). Based on duplicate analyses of two in-house
201 reference solutions USTC-Ba and ICPUS-Ba, the external precision is ≤0.04‰ for
202 $\delta^{137/134}$Ba (2SD). The $\delta^{137/134}$Ba values yielded in this study for the three USGS
203 reference materials, i.e. BCR-2, BHVO-2 and COQ-1, are in good agreement with
204 previously published values (Table 1).
205

206 ## 4. Results

207 Barium isotopic compositions are reported in Table 2 for the 0 Ma carbonatites
208 and silicate rocks from Oldoinyo Lengai (OL), and in Table 3 for Archean to
209 Cenozoic carbonatites. For reference, Ba concentrations of all samples and Mg
210 isotopic compositions of the OL samples that have been reported in previous studies
211 (Simonetti et al., 1997; Klaudius and Keller, 2006; Halama et al., 2008; Li et al., 2016)
212 are also included in Tables 2 and 3.

213 Due to the high incompatibility of Ba during mantle melting ($D^{solid/melt}$ = 0.00012;
214 Workman and Hart, 2005), preferential partition of Ba into the carbonatite melt during
215 liquid immiscibility (e.g., $D^{carbonatite\ liquid/silicate\ liquid}$ = 5.2; Veksler et al., 1998), and
216 different degrees of enrichment or depletion of Ba during magmatic crystallization,
217 the Ba concentrations of carbonatites investigated here vary considerably over more
218 than two orders of magnitude (Fig. 1). However, regardless of their highly variable Ba
219 concentrations, different localities and different ages, 17 of the 19 carbonatite samples

220 display $\delta^{137/134}$Ba values that range from −0.03 to +0.14‰, which are similar, within
221 limits of analytical uncertainties, to the range of MORBs that extends from −0.01 to
222 +0.14‰ (Nielsen et al., 2018; Fig. 1). The remaining two samples are outside the
223 range of MORBs (Fig. 1), i.e., one carbonatite from Canada (DOD 91) with a lower
224 $\delta^{137/134}$Ba value of −0.08‰ and one carbonatite from Greenland (GR74) with a higher
225 $\delta^{137/134}$Ba value of +0.23‰. The OL silicate rocks have homogeneous $\delta^{137/134}$Ba
226 values from +0.01 to +0.03‰ with an average of +0.02 ± 0.02‰ (2SD, n = 10),
227 which is identical to that of the OL carbonatites (+0.02 ± 0.02‰, 2SD, n = 5).
228

229 # 5. Discussion

230 ## 5.1. The behaviour of Ba isotopes during carbonatite petrogenesis

231 Oldoinyo Lengai has been the subject of many studies and most believe that the
232 natrocarbonatites were formed by liquid immiscibility involving a parental peralkaline
233 silicate melt at low pressures (e.g., Freestone and Hamilton, 1980; Church and Jones,
234 1995; Keller and Spettel, 1995; Dawson, 1998; Brooker and Kjarsgaard, 2011). Li et
235 al. (2016) demonstrated that the OL silicate rocks not generated by immiscibility have
236 mantle-like Mg isotopic compositions, whereas those related to carbonatites by liquid
237 immiscibility have isotopically heavier Mg (Fig. 2a). Such a difference indicates
238 significant Mg isotope fractionation during liquid immiscibility, with heavy Mg
239 isotopes preferentially partitioning into the silicate melts. By contrast, all of the OL
240 silicate rocks analyzed here have homogeneous $\delta^{137/134}$Ba values that range from
241 +0.01 to +0.03‰, all within the limits of analytical uncertainty (Fig. 2a). In addition,

there is no correlation between the $\delta^{137/134}$Ba values and the index of carbonatite magma differentiation marked by a decrease in CaO contents (Gittins and Jago, 1998; Fig. 2b). These findings suggest that even during the complex petrogenetic processes associated with the Oldoinyo Lengai magmatism, such as liquid immiscibility and crystal fractionation, little Ba isotope fractionation has taken place. The exact mechanism for the different behaviour of Mg and Ba isotopes during carbonatite magmatism is currently unclear, but may simply result from the smaller relative mass difference between ^{137}Ba and ^{134}Ba (ca. 2%) than that between ^{26}Mg and ^{24}Mg (ca. 8%).

In addition, because Ba is highly incompatible with an estimated bulk distribution coefficient $D^{solid/melt}$ of 0.00012 during mantle melting (Workman and Hart, 2005), ~99% of the Ba will enter into the melt after 1% partial melting, implying that the Ba isotopic composition of any partial melts from the mantle, including carbonatitic melts, should reflect the source composition (Nielsen et al., 2018). It thus appears that Ba isotopes remain relatively unaffected during both partial melting and liquid immiscibility, even though the Ba concentrations will be significantly changed during these processes.

5.2. Barium isotopic composition of the mantle

The similarity in $\delta^{137/134}$Ba values of most carbonatites investigated here to those of MORBs (Fig. 1) suggests that the mantle sources for both have a relatively homogeneous Ba isotopic composition. In order to estimate the average $\delta^{137/134}$Ba

264 value of the mantle sources of carbonatites, the outliers, if any, are identified through
265 statistical analysis. Using the box plot method (see NIST/SEMATECH e-Handbook of
266 Statistical Methods), three samples, i.e., DOD91, GR73 and GR74, are identified as
267 outliers (Fig. 3a).

268 Based on our data set, the average $\delta^{137/134}$Ba value of the mantle sources of the
269 parental melts to carbonatites is estimated to be +0.04 ± 0.06‰ (2SD, n = 16; Fig. 3a)
270 when the three outliers are excluded. Hence, within current analytical uncertainties,
271 the average $\delta^{137/134}$Ba value of carbonatites is indistinguishable from that of +0.05 ±
272 0.06‰ for MORBs (recalculated from Nielsen et al., 2018; Fig. 3b). This is in
273 contrast to the difference in radiogenic isotopic compositions between MORBs and
274 carbonatites (see figures in Rukhlov et al., 2015). The radiogenic isotopic
275 characteristics of some carbonatites are more closely related to those of some OIBs
276 (Bell and Tilton, 2002; Bell and Simonetti, 2010). A similarity may also exist for the
277 Ba isotope system between carbonatites and OIBs, for which an average $\delta^{137/134}$Ba
278 value of 0.02 ± 0.10‰ has been reported by Huang et al. (2015). Collectively, it
279 seems that the mantle sources for the parental melts of MORBs, OIBs and
280 carbonatites may be relatively homogeneous in terms of Ba isotopic compositions.
281 Such a characteristic implies that the terrestrial differentiation events that generated
282 the depleted and enriched mantle reservoirs (i.e., a major differentiation event during
283 the Hadean recorded by the Nd-Hf isotopes and a second one at ~3 Ga recorded by the
284 Sr-Pb isotopes; Bell and Tilton, 2002; Rukhlov et al., 2015) may not have affected the
285 Ba isotope system.

286 Our data demonstrate that the Ba isotopic compositions of the Archean to
287 present-day carbonatites investigated here overlap the range typical for modern
288 mantle-derived rocks (MORBs and OIBs). If the mantle sources of carbonatites are
289 related to subduction and recycling of oceanic lithosphere, as suggested by some
290 studies (Nelson et al., 1988; Hoernle et al., 2002; Hulett et al., 2016), we see no
291 evidence for this in terms of their Ba isotopic composition. This implies that one or
292 both of the following is true: (1) the bulk Ba isotopic composition of subducted
293 materials does not deviate greatly from the average mantle value and/or (2) subducted
294 crustal Ba is effectively homogenized upon subduction into the mantle. The first
295 possibility is in agreement with the observations that the average Ba isotopic
296 compositions of marine sediments ($\delta^{137/134}$Ba = +0.03‰) and altered oceanic crust
297 ($\delta^{137/134}$Ba = +0.07‰) overlap the average values of both carbonatites and MORBs
298 (Fig. 3).
299
300 **5.3. Local mantle Ba isotopic heterogeneity**
301 While most carbonatites display a limited variation in Ba isotopic composition,
302 there are three outliers (i.e., DOD91, GR73 and GR74; Fig. 3a). Their distinct
303 $\delta^{137/134}$Ba values may not result from surface alteration because these three samples
304 lack petrographic evidence for alteration and have Li-C-O isotopic compositions
305 similar to those of "primary" igneous carbonatites (Halama et al., 2008). In addition,
306 crustal contamination also seems unlikely because of the extremely low viscosity of
307 carbonatite melts (e.g., Genge et al., 1995). We therefore attribute the variable Ba

isotopic compositions of the three carbonatites from Canada and Greenland to local heterogeneities in the mantle.

Isotopic heterogeneity within the mantle is usually related to recycling of oceanic crustal materials (e.g., Hofmann, 2014). Although the data base is relatively small, available data show that marine sediments and altered oceanic crust (AOC) have variable $\delta^{137/134}$Ba values that range from −0.08 to +0.15‰ and from −0.07 to +0.25‰, respectively (Fig. 3b; Bridgestock et al., 2018, 2019; Nielsen et al., 2018). An even larger $\delta^{137/134}$Ba variation from −0.17 to +0.30‰ for AOC has been reported by Nan et al. (2017), and higher $\delta^{137/134}$Ba values than those presently observed in marine sediments could be expected as suspended particles in seawater display high $\delta^{137/134}$Ba values ranging from +0.19 to +0.45‰ (Horner et al., 2015; Cao et al., 2016). Hence, incorporation of recycled marine sediments and/or AOC with extreme Ba isotopic compositions in local parts of the mantle might account for the distinct $\delta^{137/134}$Ba values of the three outlier carbonatites from Canada and Greenland. If this is true, Ba isotopes could potentially be a novel tracer of crustal recycling. However, further work is needed to find out an unequivocal explanation of the observed different Ba isotopic composition (Fig. 3a) but similar Li-C-O isotopic compositions (Halama et al., 2008) between the three outliers and the other carbonatites investigated in this study.

6. Conclusions

The main conclusions from this study are:

(1) Carbonatites and associated silicate rocks from Oldoinyo Lengai have homogeneous $\delta^{137/134}$Ba values that range from +0.01 to +0.03‰, indicating insignificant Ba isotope fractionation during both silicate-carbonatite liquid immiscibility and subsequent magma differentiation. Hence, Ba isotopic composition of carbonatites could reflect that of their mantle sources.

(2) Most carbonatites from Canada, East Africa, Germany and Greenland display a limited variation in $\delta^{137/134}$Ba values ranging from −0.03 to +0.09‰, suggesting that the mantle sources of carbonatites have a relatively homogeneous Ba isotopic composition. The spatial distribution of the 16 carbonatites we have measured suggests that their mantle sources have an average $\delta^{137/134}$Ba value of +0.04 ± 0.06‰ (2SD), similar to those of MORBs and OIBs. Therefore, the mantle sources for the parental melts of MORBs, OIBs and carbonatites are likely to be relatively homogeneous in terms of Ba isotopic compositions.

(3) The distinct $\delta^{137/134}$Ba values of the three outlier carbonatites might reflect the incorporation of marine sediments and/or altered oceanic crust with extreme Ba isotopic compositions in their mantle sources. On the basis of these observations, Ba isotopes may potentially be a novel tracer of crustal recycling.

Acknowledgments

We thank J. Keller and J. Klaudius for sharing samples. The constructive comments from three anonymous reviewers and efficient handling from the editor Fang-Zhen Teng are greatly appreciated. This work is financially supported by the

National Natural Science Foundation of China (41573002, 41873005, 41630206) and by the Natural Sciences and Engineering Research Council of Canada.

References

Barker D. S. (1996) Consequences of recycled carbon in carbonatites. *Can. Mineral.* **34**, 373–387.

Bell K. and Keller J. (1995) Carbonatite Volcanism: Oldoinyo Lengai and the Petrogenesis of Natrocarbonatites. IAVECI Proceedings in Volcanology 4. Springer-Verlag, Berlin. 210p.

Bell K. and Simonetti A. (1996) Carbonatite magnetism and plume activity: implications from the Nd, Pb and Sr isotope systematics of Oldoinyo Lengai. *J. Petrol.* **37**, 1321–1339.

Bell K, Kjarsgaard B. A. and Simonetti A. (1998) Carbonatites – into the twenty-first century. *J. Petrol.* **39**, 1839–1845.

Bell K. and Tilton G. R. (2001) Nd, Pb and Sr isotopic compositions of East African Carbonatites: evidence for mantle mixing and plume inhomogeneity. *J. Petrol.* **42**, 1927–1945.

Bell K. and Tilton G. R. (2002) Probing the mantle: the story from carbonatites. *EOS Transactions, AGU 83*, **273**, 276–277.

Bell K. and Simonetti A. (2010) Source of parental melts to carbonatites – critical isotopic constraints. *Miner. Petrol.* **98**, 77–89.

374 Bizimis M., Salters V. J. M. and Dawson J. B. (2003) The brevity of carbonatite
375 sources in the mantle: evidence from Hf isotopes. *Contrib. Mineral. Petrol.* **145**,
376 281–300.
377 Bridgestock L., Hsieh Y.-T., Porcelli D., Homoky W. B., Bryan A. and Henderson G.
378 M. (2018) Controls on the barium isotope compositions of marine sediments.
379 *Earth Planet. Sci. Lett.* **481**, 101–110.
380 Bridgestock L., Hsieh Y.-T., Porcelli D. and Henderson G. M. (2019) Increased export
381 production during recovery from the Paleocene–Eocene thermal maximum
382 constrained by sedimentary Ba isotopes. *Earth Planet. Sci. Lett.* **510**, 53–63.
383 Brooker R. A. and Kjarsgaard B. A. (2011) Silicate–carbonate liquid immiscibility
384 and phase relations in the system SiO_2–Na_2O–Al_2O_3–CaO–CO_2 at 0.1–2.5 GPa
385 with application to carbonatite genesis. *J. Petrol.* **52**, 1281–1305.
386 Bullen T. and Chadwick O. (2016) Ca, Sr and Ba stable isotopes reveal the fate of soil
387 nutrients along a tropical climosequence in Hawaii. *Chem. Geol.* **422**, 25–45.
388 Cao Z., Siebert C., Hathorne E. C., Dai M. and Frank M. (2016) Constraining the
389 oceanic barium cycle with stable barium isotopes. *Earth Planet. Sci. Lett.* **434**,
390 1–9.
391 Charbonnier Q., Moynier F. and Bouchez J. (2018) Barium isotope cosmochemistry
392 and geochemistry. *Sci. Bull.* **63**, 385–394.
393 Church A. A. and Jones A. P. (1995) Silicate-carbonate immiscibility at Oldoinyo
394 Lengai. *J. Petrol.* **36**, 869–889.

395 Dawson J. B. (1998) Peralkaline nephelinite–natrocarbonatite relationships at
396 Oldoinyo Lengai, Tanzania. *J. Petrol.* **39**, 2077–2094.
397 Deines P. (1989) Stable isotope variations in carbonatites. In Carbonatites: Genesis
398 and Evolution (ed. K. Bell). Unwin Hyman, London. pp. 301–359.
399 Demény A., Sitnikova, M. A. and Karchevsky P. I. (2004) Stable C and O isotope
400 compositions of carbonatite complexes of the Kola Alkaline Province:
401 phoscorite-carbonatite relationships and source compositions. In Phoscorites and
402 Carbonatites from Mantle to Mine: the Key Example of the Kola Alkaline
403 Province (eds. F. Wall and A. N. Zaitsev). The Mineralogical Society Series 10, pp.
404 407–431.
405 Ernst R. E. and Bell K. (2010) Large igneous provinces (LIPs) and carbonatites.
406 *Miner. Petrol.* **98**, 55–76.
407 Eugster O., Tera F. and Wasserburg G. J. (1969) Isotopic analyses of barium in
408 meteorites and in terrestrial samples. *J. Geophys. Res.* **74**, 3897–3908.
409 Freestone I. C. and Hamilton D. L. (1980) The role of liquid immiscibility in the
410 genesis of carbonatites – An experimental study. *Contrib. Mineral. Petrol.* **73**,
411 105–117.
412 Genge M. J., Price G. D. and Jones A. P. (1995) Molecular dynamics simulation of
413 $CaCO_3$ melts to mantle pressures and temperatures: implications for carbonatite
414 magmas. *Earth Planet. Sci. Lett.* **131**, 225–238.
415 Gittins J. and Jago B. C. (1998) Differentiation of natrocarbonatite magma at
416 Oldoinyo Lengai volcano, Tanzania. *Mineral. Mag.* **62**, 759–768.

417 Halama R., Vennemann T. W., Siebel W. and Markl G. (2005) The Grønnedal–Ika
418 carbonatite-syenite complex, South Greenland: carbonatite formation by liquid
419 immiscibility. *J. Petrol.* **46**, 191–217.
420 Halama R., McDonough W. F., Rudnick R. L., Keller J. and Klaudius J. (2007) The Li
421 isotopic composition of Oldoinyo Lengai: nature of the mantle sources and lack of
422 isotopic fractionation during carbonatite petrogenesis. *Earth Planet. Sci. Lett.* **254**,
423 77–89.
424 Halama R., McDonough W. F., Rudnick R. L. and Bell K. (2008) Tracking the lithium
425 isotopic evolution of the mantle using carbonatites. *Earth Planet. Sci. Lett.* **265**,
426 726–742.
427 Hoefs J. (2018) Stable isotope geochemistry (eighth edition). Springer, Berlin. 437p.
428 Hoernle K., Tilton G., Le Bas M. J., Duggen S. and Garbe-Schönberg D. (2002)
429 Geochemistry of oceanic carbonatites compared with continental carbonatites:
430 mantle recycling of oceanic crustal carbonate. *Contrib. Mineral. Petrol.* **142**,
431 520–542.
432 Hofmann A. W. (2014) Sampling mantle heterogeneity through oceanic basalts:
433 isotopes and trace element. In Treatise on Geochemistry, vol. 3, The mantle and
434 core (second ed.) (ed. R.W. Carlson). Elsevier, Oxford. pp. 67–101.
435 Horner T. J., Kinsley C. W. and Nielsen S. G. (2015) Barium-isotopic fractionation in
436 seawater mediated by barite cycling and oceanic circulation. *Earth Planet. Sci.*
437 *Lett.* **430**, 511–522.

438 Huang F., Nan X.-Y., Yu H.-M., Huang S.-C. and Huang J. (2015) Barium isotope
439 compositions of igneous rocks. *Goldschmidt Abstr.* 1331.
440 Hulett S. R. W., Simonetti A., Rasbury E. T. and Hemming N. G. (2016) Recycling of
441 subducted crustal components into carbonatite melts revealed by boron isotopes.
442 *Nat. Geosci.* **9**, 904–909.
443 Keller J. and Kraft M. (1990) Effusive natrocarbonatite activity of Oldoinyo Lengai,
444 June 1988. *Bull. Volcanol.* **52**, 629–645.
445 Keller J. and Hoefs J. (1995) Stable isotope characteristics of recent natrocarbonatites
446 from Oldoinyo Lengai. In Carbonatite Volcanism: Oldoinyo Lengai and the
447 Petrogenesis of Natrocarbonatites (eds. K. Bell and J. Keller). Springer-Verlag,
448 Berlin. pp. 113–123.
449 Keller J. and Spettel B. (1995) The trace element composition and petrogenesis of
450 natrocarbonatites. In Carbonatite volcanism: Oldoinyo Lengai and the
451 Petrogenesis of Natrocarbonatite (eds. K. Bell and J. Keller). Springer-Verlag,
452 Berlin. pp. 70–86.
453 Klaudius J. and Keller J. (2006) Peralkaline silicate lavas at Oldoinyo Lengai,
454 Tanzania. *Lithos* **91**, 173–190.
455 Li W.-Y., Teng F.-Z., Halama R., Keller J. and Klaudius J. (2016) Magnesium isotope
456 fractionation during carbonatite magmatism at Oldoinyo Lengai, Tanzania. *Earth*
457 *Planet. Sci. Lett.* **444**, 26–33.

458 Mitchell R. H. and Dawson J. B. (2012) Carbonate-silicate immiscibility and
459 extremely peralkaline silicate glasses from Nasira cone and recent eruptions at
460 Oldoinyo Lengai Volcano, Tanzania. *Lithos* **152**, 40–46.
461 Nan X., Wu F., Zhang Z., Hou Z., Huang F. and Yu H. (2015) High-precision barium
462 isotope measurements by MC-ICP-MS. *J. Anal. At. Spectrom.* **30**, 2307–2315.
463 Nan X., Yu H. and Gao Y. (2017) Barium isotope composition of altered oceanic crust
464 from IODP Site 1256 at the East Pacific Rise. *AGU Abstr.* V33C-0534.
465 Nan X.-Y., Yu H.-M., Rudnick R. L., Gaschnig R. M., Xu J., Li W.-Y., Zhang Q., Jin
466 Z.-D., Li X.-H. and Huang F. (2018) Barium isotopic composition of the upper
467 continental crust. *Geochim. Cosmochim. Acta* **233**, 33–49.
468 Nelson D. R., Chivas A. R., Chappell B. W. and McCulloch M. T. (1988)
469 Geochemical and isotopic systematics in carbonatites and implications for the
470 evolution of ocean-island sources. *Geochim. Cosmochim. Acta* **52**, 1–17.
471 Nielsen S. G., Horner T. J., Pryer H. V., Blusztajn J., Shu Y., Kurz M. D. and Le Roux
472 V. (2018) Barium isotope evidence for pervasive sediment recycling in the upper
473 mantle. *Sci. Adv.* **4**, eaas8675.
474 NIST/SEMATECH e-Handbook of Statistical Methods. The chapter 7.1.6. What are
475 outliers in the data? https://www.itl.nist.gov/div898/handbook/prc/section1/prc16.htm.
476 Peterson T. D. (1990) Petrology and genesis of natrocarbonatite. *Contrib. Mineral.*
477 *Petrol.* **105**, 143–155.

478 Plank T. (2014) The chemical composition of subducting sediments. In Treatise on
479 Geochemistry, vol. 4, The crust (second ed.) (ed. R. L. Rundick). Elsevier, Oxford.
480 pp. 607–629.
481 Potter N. J., Kamenetsky V. S., Simonetti A. and Goemann K. (2017) Different types
482 of liquid immiscibility in carbonatite magmas: A case study of the Oldoinyo
483 Lengai 1993 lava and melt inclusions. *Chem. Geol.* **455**, 376–384.
484 Ray J. S., Ramesh R. and Pande K. (1999) Carbon isotopes in Kerguelen
485 plume-derived carbonatites: evidence for recycled inorganic carbon. *Earth Planet.*
486 *Sci. Lett.* **170**, 205–214.
487 Rudge J. F., Reynolds B. C. and Bourdon B. (2009) The double spike toolbox. *Chem.*
488 *Geol.* **265**, 420–431.
489 Rudnick R. L. and Gao S. (2014) Composition of the continental crust. In Treatise on
490 Geochemistry, vol. 4, The crust (second ed.) (ed. R. L. Rundick). Elsevier, Oxford.
491 pp. 1–51.
492 Rukhlov A. S., Bell K. and Amelin Y. (2015) Carbonatites, isotopes and evolution of
493 the subcontinental mantle: An overview. In Symposium on Strategic and Critical
494 Materials Proceedings (eds. G. J. Simandl and M. Neetz). British Columbia
495 Geological Survey Paper 2015-3. pp. 39–64.
496 Salters V. J. M. and Stracke A. (2004) Composition of the depleted mantle. *Geochem.*
497 *Geophys. Geosyst.* **5**, Q05B07, doi:10.1029/2003GC000597.

498 Schleicher H., Keller J. and Kramm U. (1990) Isotope studies on alkaline volcanics
499 and carbonatites from the Kaisertuhl, Federal Republic of Germany. *Lithos* **26**,
500 21–35.
501 Simonetti A., Bell K. and Shrady C. (1997) Trace- and rare-earth-element
502 geochemistry of the June 1993 natrocarbonatite lavas, Oldoinyo Lengai
503 (Tanzania): implications for the origin of carbonatite magmas. *J. Volcanol.*
504 *Geotherm. Res.* **75**, 89–106.
505 Sun S.-S. and McDonough W. F. (1989) Chemical and isotopic systematics of oceanic
506 basalts: implications for mantle composition and processes. In Magmatism in the
507 Ocean Basins (eds. A. D. Saunders and M. J. Norry). Geological Society, London.
508 pp. 313–345.
509 Teng F.-Z., Watkins J. and Dauphas N. (2017) Non-traditional stable isotopes. *Rev.*
510 *Mineral. Geochem.* **82**, 885p.
511 Tilton G. R. and Bell K. (1994) Sr–Nd–Pb isotope relationship in Late Archean
512 carbonatites and alkaline complexes: applications to the geochemical evolution of
513 Archean mantle. *Geochim. Cosmochim. Acta* **58**, 3145–3154.
514 Veksler I. V., Petibon C., Jenner G. A., Dorfman A. M. and Dingwell D. B. (1998)
515 Trace element partitioning in immiscible silicate-carbonate liquid systems: an
516 initial experimental study using a centrifuge autoclave. *J. Petrol.* **39**, 2095–2104.
517 von Allmen K., Böttcher M. E., Samankassou E. and Nägler T. F. (2010) Barium
518 isotope fractionation in the global barium cycle: First evidence from barium
519 minerals and precipitation experiments. *Chem. Geol.* **277**, 70–77.

520 Woolley A. R. and Kempe D. R. C. (1989) Carbonatites: Nomenclature, average
521 chemical compositions and element distribution. In Carbonatites: Genesis and
522 Evolution (ed. K. Bell). Unwin Hyman, London. pp. 1–14.
523 Woolley A. R. and Kjarsgaard B. A. (2008) Carbonatite occurrences of the world: map
524 and database. *Geol. Surv. Can.* Open File 5796, 10.4095/225115.
525 Workman R. K. and Hart S. R. (2005) Major and trace element composition of the
526 depleted MORB mantle (DMM). *Earth Planet. Sci. Lett.* **231**, 53–72.
527 Zeng Z., Li X., Liu Y., Huang F. and Yu H.-M. (2019) High-precision barium isotope
528 measurements of carbonates by MC-ICP-MS. *Geostand. Geoanal. Res.* **43**,
529 291–300.
530

Table 1

Barium isotopic compositions of reference materials

Standard	Description	$\delta^{137/134}$Ba(‰)	2SD(‰)[a]	Reference
BCR-2	Basalt, Columbia	+0.02	0.03	
Duplicate[b]	River, USA	+0.06	0.03	
Duplicate		+0.05	0.04	
Duplicate		+0.04	0.03	
Duplicate		+0.02	0.04	
Average	(*n* = 5)	+0.04	0.04	This study
		+0.05	0.04	Nan et al. (2015)
		+0.05	0.03	Nan et al. (2018)
BHVO-2	Basalt, Hawaii, USA	+0.01	0.03	
Duplicate		+0.04	0.03	
Duplicate		+0.02	0.04	
Average	(*n* = 3)	+0.02	0.03	This study
		+0.05	0.03	Nan et al. (2015)
		+0.05	0.04	Bullen and Chadwich (2016)
COQ-1	Carbonatite, Oka	+0.06	0.03	
Duplicate	complex, Canada	+0.08	0.03	
Duplicate		+0.07	0.04	
Duplicate		+0.07	0.04	
Average	(*n* = 4)	+0.07	0.02	This study
		+0.08	0.04	Zeng et al. (2019)

[a] 2SD = two times the standard deviation of n repeat measurements.

[b] Duplicate = repeat column chemistry and measurement of different aliquots of a stock solution.

536 **Table 2**

537 Barium isotopic compositions and selected geochemical parameters of the natrocarbonatites and

538 silicate rocks from Oldoinyo Lengai (OL), Tanzania.

Sample ID	Rock type	Ba(μg/g)[a]	$\delta^{137/134}$Ba(‰)	2SD(‰)[b]	δ^{26}Mg(‰)[c]	2SD(‰)[c]
OL carbonatites						
OL2	Natrocarbonatite	13,430	+0.03	0.03	+0.31	0.08
OL7	Natrocarbonatite	14,330	+0.03	0.03	+0.37	0.10
OL123	Natrocarbonatite	11,280	+0.01	0.03	+0.19	0.10
Duplicate[d]			+0.02	0.04		
OL148	Natrocarbonatite	15,040	+0.01	0.03	+0.16	0.10
Duplicate			+0.01	0.04		
OL259	Natrocarbonatite	13,790	+0.03	0.03	+0.13	0.10
OL silicate rocks not generated by liquid immiscibility						
OL247	Nephelinite	1431	+0.02	0.03	−0.14	0.10
OL440	Phonolite	1440	+0.03	0.03	−0.10	0.07
OL442	Phonolite	1669	+0.01	0.03	−0.11	0.07
Duplicate			+0.01	0.04		
OL450	Phonolite	1523	+0.01	0.03	−0.12	0.11
OL503	Phonolite	1614	+0.02	0.03	−0.15	0.11
OL803	Nephelinite	1612	+0.02	0.03	−0.13	0.10
Duplicate			+0.02	0.04		
OL822	Phonolite	1532	+0.03	0.03	−0.25	0.09
OL silicate rocks related to the carbonatites by liquid immiscibility						
OL624	Nephelinite	1564	+0.02	0.03	−0.06	0.09
OL788	Nephelinite	1970	+0.01	0.03	+0.07	0.11
OL804	Nephelinite	2654	+0.01	0.03	+0.09	0.08
Duplicate			+0.01	0.04		

539 [a] Data from Simonetti et al. (1997) and Klaudius and Keller (2006).

540 [b] 2SD = two times the standard deviation of n (n >20) repeat measurements of the in-house reference solutions

541 during an analytical session.

542 [c] Data from Li et al. (2016).

543 [d] Duplicate = repeat column chemistry and measurement of different aliquots of a stock solution.

544

Table 3

Barium concentrations and isotopic compositions of carbonatites from Canada, East Africa, Germany, and Greenland.

Sample ID	Rock type	Age(Ma)[a]	Ba(μg/g)[a]	$\delta^{137/134}$Ba(‰)	2SD(‰)[b]
Canada					
DOD77	Calcite carbonatite	2680	985	−0.03	0.04
DOD91	Silicocarbonatite	2680	806	−0.07	0.04
Duplicate[c]				−0.08	0.04
LSC20	Calcite carbonatite	2680	706	+0.08	0.04
Duplicate				+0.09	0.04
LSC108	Calcite carbonatite	2680	1472	+0.09	0.04
Duplicate				+0.09	0.04
East Africa					
N1295	Calcite carbonatite	138	3920	+0.02	0.04
PH212	Calcite carbonatite	116	452	+0.05	0.04
PH213	Calcite carbonatite	116	530	+0.04	0.04
SU103	Calcite carbonatite	40	366	+0.05	0.04
DU365	Ferrocarbonatite	40	799	+0.05	0.04
HB	Calcite carbonatite	13	4454	+0.01	0.04
Germany					
K5	Calcite carbonatite	17	1319	+0.03	0.04
Greenland					
GR46	Calcite carbonatite	1300	405	+0.05	0.04
GR73	Calcite carbonatite	1300	91	+0.13	0.04
Duplicate				+0.15	0.04
GR74	Calcite carbonatite	1300	66	+0.22	0.03
Duplicate				+0.23	0.03

[a] Data from Halama et al. (2008) and references therein.

[b] 2SD = two times the standard deviation of n (n >20) repeat measurements of the in-house reference solutions during an analytical session.

[c] Duplicate = repeat column chemistry and measurement of different aliquots of a stock solution.

552 **Figure captions**

553 **Fig. 1.** $\delta^{137/134}$Ba vs. Ba (μg/g) for carbonatites from Canada, East Africa (including
554 Oldoinyo Lengai (OL)), Germany and Greenland. Data for silicate rocks from
555 Oldoinyo Lengai are also shown. The gray area marks distribution of data from
556 mid-ocean ridge basalts (MORBs) reported in Nielsen et al. (2018). The $\delta^{138/134}$Ba
557 values reported in Nielsen et al. (2018) have been recalculated here to $\delta^{137/134}$Ba
558 values, i.e. $\delta^{137/134}Ba = 0.75 \times \delta^{138/134}Ba$ (Horner et al., 2015). Error bars represent
559 2SD uncertainties. Data are from Tables 2 and 3.

560

561 **Fig. 2.** (a) $\delta^{137/134}$Ba vs. δ^{26}Mg for silicate rocks from Oldoinyo Lengai (OL); (b)
562 $\delta^{137/134}$Ba vs. CaO (wt%) for carbonatites from OL. Data are from Table 2, and the
563 CaO contents from Simonetti et al. (1997).

564

565 **Fig. 3.** (a) Histogram of $\delta^{137/134}$Ba values for carbonatites from Canada, East Africa
566 (including Oldoinyo Lengai), Germany and Greenland. The red circles represent the
567 three outliers identified using the box plot method (see NIST/SEMATECH
568 e-Handbook of Statistical Methods). The gray band and vertical red line represent
569 the range and estimated average $\delta^{137/134}$Ba value for the mantle sources of
570 carbonatites (i.e., +0.04 ± 0.06‰, 2SD), excluding the three outliers. Data are from
571 Tables 2 and 3. (b) Histogram of $\delta^{137/134}$Ba values for MORBs (Nielsen et al., 2018).
572 The black horizontal lines and red vertical lines respectively represent the range and
573 the average of $\delta^{137/134}$Ba values for marine sediments (Bridgestock et al., 2018, 2019;

574 Nielsen et al., 2018) and altered oceanic crust (AOC; Nielsen et al., 2018). The
575 published $\delta^{138/134}Ba$ values have been recalculated here to $\delta^{137/134}Ba$ values, i.e.
576 $\delta^{137/134}Ba = 0.75 \times \delta^{138/134}Ba$ (Horner et al., 2015).

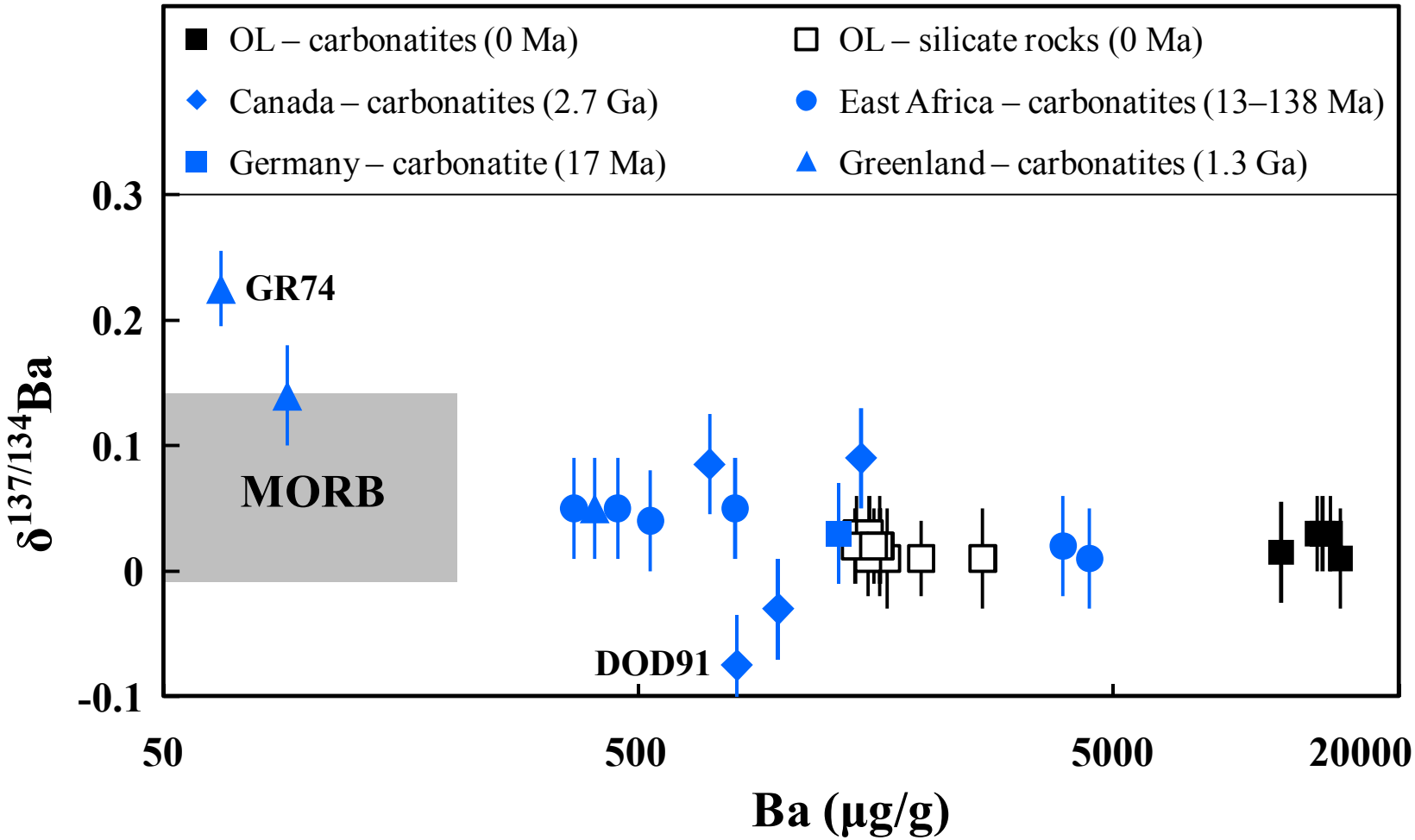
OL – carbonatites (0 Ma)
OL – silicate rocks (0 Ma)
Canada – carbonatites (2.7 Ga)
East Africa – carbonatites (13–138 Ma)
Germany – carbonatite (17 Ma)
Greenland – carbonatites (1.3 Ga)
0.3
0.2
0.1
0
-0.1
δ137/134Ba
GR74
MORB
DOD91
50
500
5000
20000
Ba (µg/g)

Fig. 1

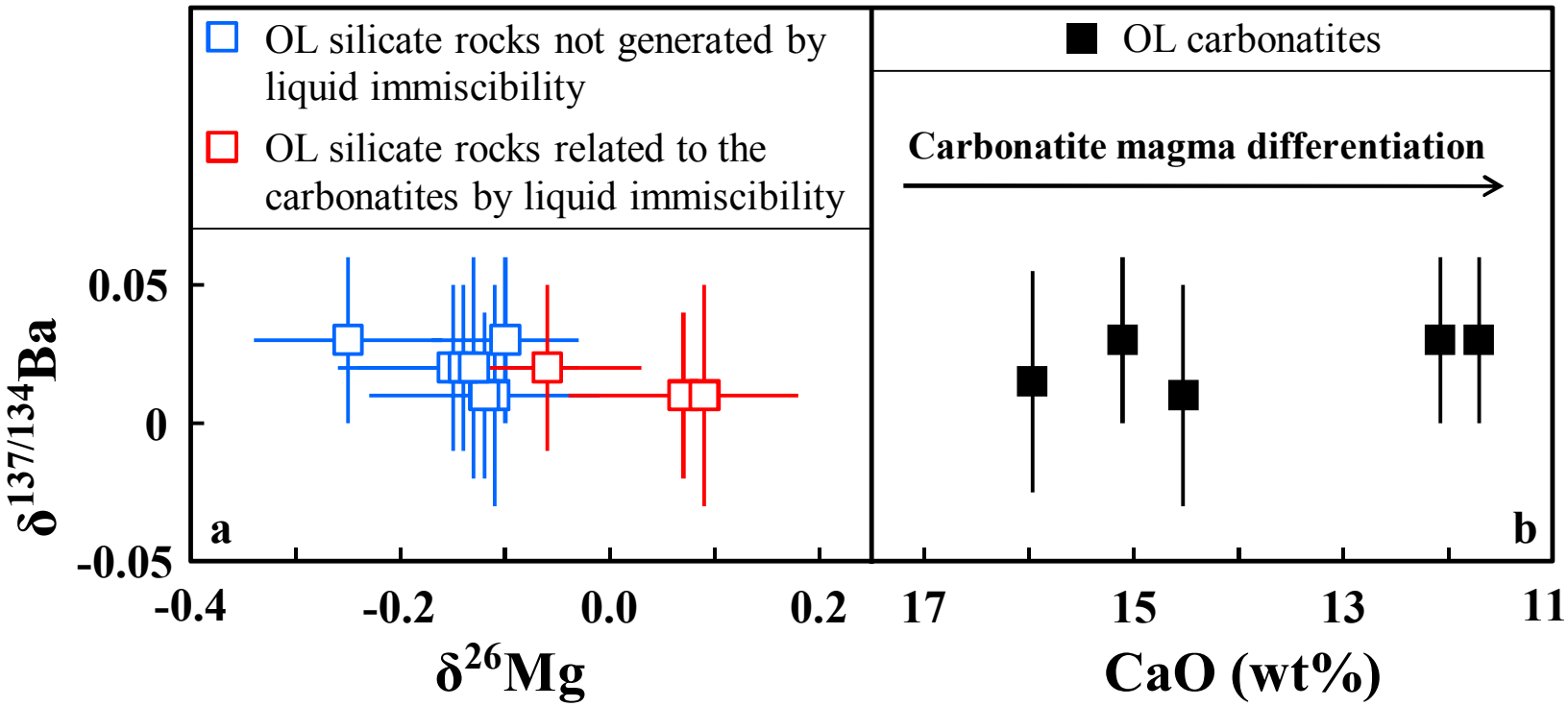
OL silicate rocks not generated by liquid immiscibility
OL silicate rocks related to the carbonatites by liquid immiscibility
OL carbonatites
Carbonatite magma differentiation
0.05
0
-0.05
δ137/134Ba
a
b
-0.4
-0.2
0.0
0.2
17
15
13
11
δ26Mg
CaO (wt%)

Fig. 2

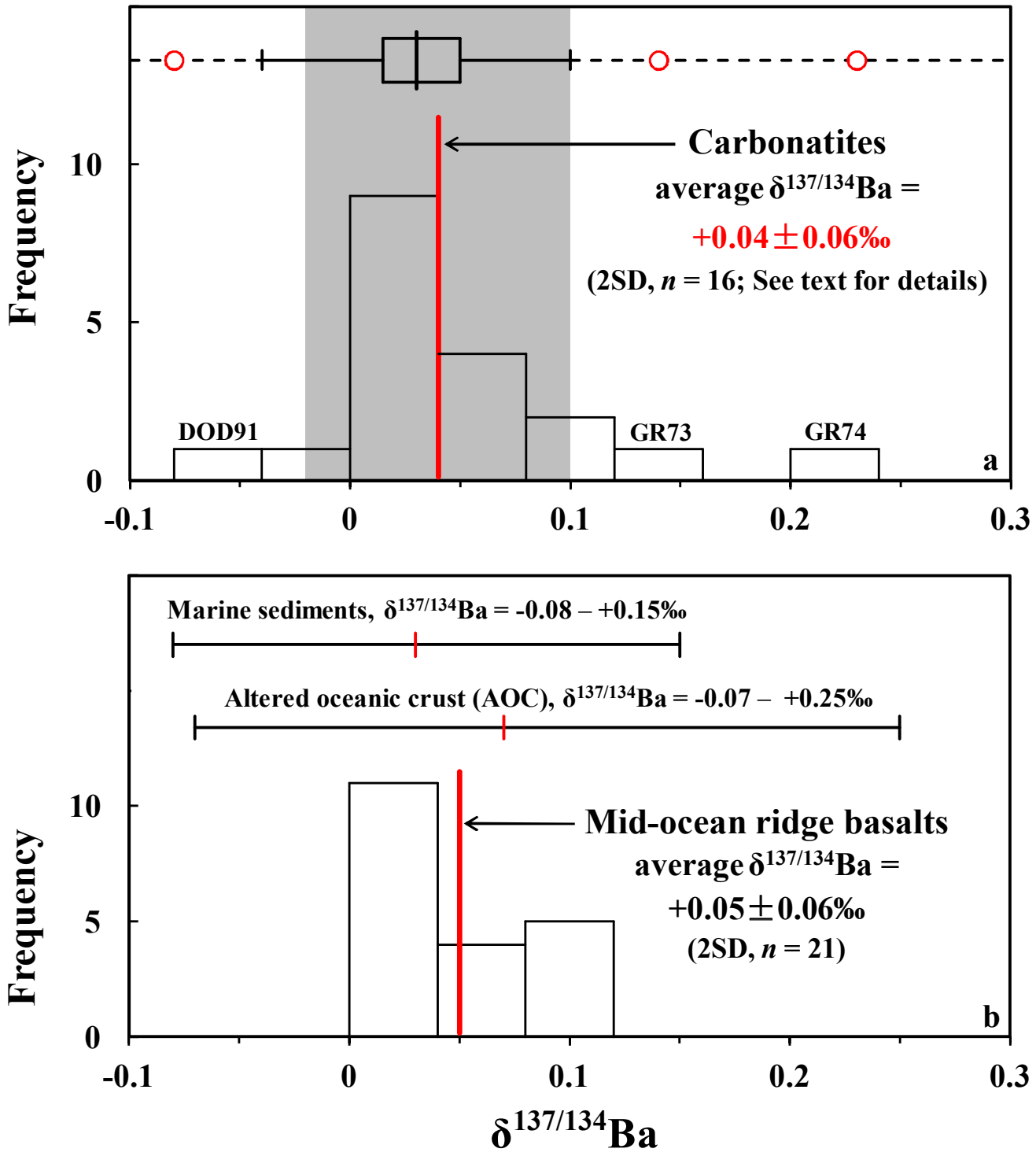
Carbonatites
average δ137/134Ba =
+0.04±0.06‰
(2SD, n = 16; See text for details)
DOD91
GR73
GR74
a
Frequency
10
5
0
-0.1
0
0.1
0.2
0.3
Marine sediments, δ137/134Ba = -0.08 – +0.15‰
Altered oceanic crust (AOC), δ137/134Ba = -0.07 – +0.25‰
Mid-ocean ridge basalts
average δ137/134Ba =
+0.05±0.06‰
(2SD, n = 21)
b
δ137/134Ba

Fig. 3